

Evidence for a Liquid-to-Crystal Phase Transition in a Classical, Two-Dimensional Sheet of Electrons

C. C. Grimes and G. Adams

Bell Laboratories, Murray Hill, New Jersey 07974

(Received 17 January 1979)

Experimental evidence is presented for an electron-liquid to electron-crystal phase transition in a sheet of electrons on a liquid-He surface. The phase transition has been studied for electron areal densities from $3 \times 10^8 \text{ cm}^{-2}$ to $9 \times 10^8 \text{ cm}^{-2}$ and has yielded melting temperatures between 0.35 and 0.65 K. The phase transition occurs at $\Gamma = 137 \pm 15$, where Γ is a measure of the ratio of potential energy to kinetic energy per electron.

We report the first experimental determination of a portion of the phase boundary for the electron-liquid to electron-crystal phase transition in a classical, two-dimensional (2D) Coulomb system. The 2D system that we have studied consists of a monolayer of electrons trapped on the surface of liquid helium. This electron layer is a nearly ideal 2D Coulomb system for such a study because the areal density of electrons can be varied over several orders of magnitude and the He surface is inherently clean (i.e., free of traps and scattering centers).

Historically, Wigner first calculated in 1934 that an electron-liquid to electron-solid phase transition should occur in the 3D Fermi system at *low* densities.¹ Crandall and Williams noted that the analogous phase transition should occur in the classical 2D electron system at sufficiently *high* electron areal densities.² The thermodynamic state of a classical Coulomb system is determined by the quantity Γ which is a measure of the ratio of Coulomb potential energy to kinetic energy per particle. For the classical 2D electron system this ratio becomes $\Gamma = \pi^{1/2} N_s^{1/2} e^2 / k_B T$, where N_s is the electron areal density and T is the system temperature. For $\Gamma < 1$ the kinetic energy predominates and the system behaves like an electron gas. At intermediate densities $1 \lesssim \Gamma \lesssim 100$, the electron motions become highly correlated or liquidlike. At high densities $\Gamma \gtrsim 100$, the Coulomb potential energy predominates and the electrons are expected to undergo a phase transition to form a periodic crystalline array. An experimental determination of this phase boundary is of interest to provide guidance for the difficult calculations and numerical experiments that are emerging for the melting transition in the classical 2D Coulomb solid.

In this Letter we briefly describe our experimental technique and apparatus. We then summarize our experimental results and compare our phase boundary with the results of computer

experiments by others.

An excess electron outside a free surface of liquid helium can be bound just above the surface in a potential well formed by the combination of the long-range classical image potential and the short-range repulsive barrier to penetration into the liquid. While the electron is bound in the direction normal to the surface with a binding energy of 0.7 meV, it remains free to move parallel to the surface. For a bound electron the spatial extent of its wave function normal to the surface is $\approx 10^{-6} \text{ cm}$ while the interelectron spacing is typically $5 \times 10^{-5} \text{ cm}$; so the electrons interact like point charges. The experimentally accessible range of areal densities is approximately $10^5 \lesssim N_s \lesssim 10^9 \text{ cm}^{-2}$ which at a representative temperature of 0.5 K corresponds to $2 \lesssim \Gamma \lesssim 200$.³ Also, at $N_s = 10^9$ Fermi energy is 0.03 K, which is small relative to our experimental temperatures, so that the electrons obey classical (Boltzmann) statistics.

To detect the presence of the electron crystal, we have employed a variant of a novel experiment proposed by Shikin⁴ and Monarkha and Shikin.⁵ Shikin suggested that when the electrons have formed a crystal, then driving the crystal up and down against the He surface with a uniform, perpendicular rf electric field should produce a series of resonances due to excitation of standing capillary waves (ripples) on the He surface. Standing capillary waves will be resonantly excited when an integral number of capillary-wave wavelengths equals the spacing between rows of electrons in the crystal and the driving frequency matches the capillary-wave frequency for that wavelength. That is, the resonances occur when the driving frequency satisfies the capillary-wave dispersion relation $\omega^2 = (\alpha/\rho) G_n^3$ with G_n a reciprocal-lattice vector of the electron lattice. Here α and ρ are, respectively, the surface-tension coefficient and density of liquid He. For a triangular lattice the resonance frequen-

cies are given by

$$\nu_n = 2^{5/4} 3^{-3/8} \pi^{1/2} (\alpha/\rho)^{1/2} N_s^{3/4} n^{3/4}, \quad (1)$$

where $n = i^2 + j^2 + ij$ and i and j are zero or integers so that $n = 1, 3, 4, 7, \dots$.⁵ In fact, we believe that we have not detected the Shikin modes, but rather have seen coupled plasmon-rippion modes which are described by Fisher, Halperin, and Platzman.⁶ The coupled plasmon-rippion modes involve nonuniform horizontal motions of the electrons rather than the uniform vertical motions of the Shikin modes; therefore they couple to nonuniform electric fields *parallel* to the He surface. These modes have absorption strengths much larger than those expected for the Shikin modes, and the lowest resonances occur at frequencies which are significantly perturbed from (1).

In the experiment, we look for the appearance of the coupled resonances as we increase Γ by varying T and N_s . The experimental cell consists of a pair of 5-cm-diam circular capacitor plates, one of which is located about 0.2 cm above the helium surface and contains a tiny filament at its center. The lower capacitor plate is submerged beneath the He surface a distance d which is typically about 0.1 cm. This plate has the rf-driven element⁷ at its center surrounded by an annular guard ring. A metal confining ring at the He surface completes the experimental cell. The guard ring is maintained at ground potential as is the time average potential of the driven element. This element is connected to a swept-frequency broadband rf bridge spectrometer which drives it with an rf potential of about 1 mV (rms). The experimental cell is enclosed in a vacuum-tight copper can and attached to a conventional ³He refrigerator. The liquid-He level in the cell is adjusted by condensing He into it. Appropriate negative potentials are applied to the filament, upper capacitor plate, and the confining ring, and then the filament is briefly heated to deposit electrons on the He surface. Under typical operating conditions, the surface is fully charged and so the potential of the electron layer is the same as the potential V_u of the upper capacitor plate. The value of N_s is fixed by the values of V_u and d , and since the resonances are excited primarily in the central region of the cell, N_s is quite uniform.⁸ (Note that the positive compensating charge resides on the submerged electrode.) An audiofrequency potential of about 20 mV (rms) superposed on the potential applied to the confining ring modulates N_s by an infinitesimal amount. Synchronous detection at the modulation frequency

then yields experimental traces that are plots of dR/dN_s versus the rf frequency ν at a fixed value of N_s and T . Here R is the real part of the impedance of the driven element. The experimental signal dR/dN_s is proportional to $-d\sigma_{\perp}(\nu)/dN_s$, where $\sigma_{\perp}(\nu)$ is the frequency-dependent electron-layer conductivity normal to the He surface. A sequence of traces at different values of T with $N_s = (4.4 \pm 0.4) \times 10^8 \text{ cm}^{-2}$ is shown in Fig. 1.

The lowest-temperature trace in Fig. 1 displays four prominent resonances which we have arbitrarily labeled W , X , Y , and Z . Their measured frequencies are 10.2, 12.3, 31.4, and 39.4 ± 0.2 MHz, respectively. At $N_s = 4.4 \times 10^8 \text{ cm}^{-2}$, the calculated frequencies of the three lowest modes using (1) are 15.1, 31.1, and 38.6 MHz. Thus the Y and Z resonances are within 2% of ν_3 and ν_4 , respectively. Furthermore, the observed frequencies of the Y and Z resonances are essentially independent of T (except very near melting) and of E_{\perp} , the electric field pressing the electrons against the surface, and both frequencies vary with electron density as $N_s^{3/4}$ in agreement with (1). Resonances W and X behave in a more complicated manner. Both resonances move approximately linearly to higher frequencies with increasing T and to lower frequencies with increasing E_{\perp} . The frequencies of W and X , which have been studied only in the limited interval $300 \lesssim E_{\perp} \lesssim 550$ V/cm, when extrapolated to $E_{\perp} = 0$ are nearly independent of T and both fall close to ν_1 . Fisher, Halperin, and Platzman have proposed that the dependences of the resonance frequencies on T

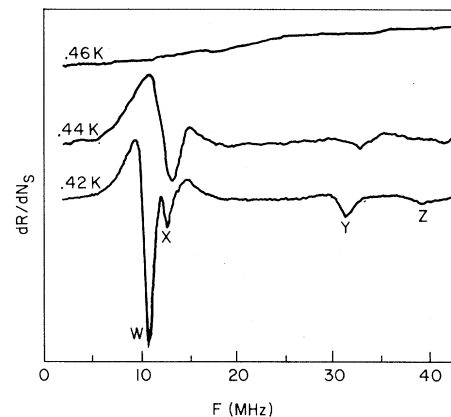


FIG. 1. Experimental traces displaying the sudden appearance with decreasing temperature of coupled plasmon-rippion resonances. The resonances only appear below 0.457 K where the sheet of electrons has crystallized into a triangular lattice.

and E_{\perp} are characteristic of coupled plasmon-rippion modes.⁶ They find that the coupled plasmon-rippion spectrum contains a series of resonances at or below each of the "bare" resonances. They identify the W and X resonances as the two lowest modes of the $n=1$ series, and they find good agreement between their calculated frequencies and those we have measured. The observed spectrum with its N_s and E_{\perp} dependence provides strong evidence that the resonances are due to coupled plasmon-rippion modes excited by a triangular electron lattice of areal density N_s .⁹

The resonances in Fig. 1 appear rather abruptly when T is below a threshold value of $\approx 0.457 \pm 0.005$ K. A reasonably precise value of the threshold temperature T_m can be obtained by plotting the peak-to-peak amplitudes of the strongest resonances versus T and extrapolating to zero amplitude. Taking T_m to be the electron-liquid to electron-crystal phase-transition temperature, we can establish the phase boundary in the N_s - T plane by repeating the T_m determination at a number of different values of N_s . Figure 2 presents a $N_s^{1/2}$ vs T_m plot obtained in several different runs using several different values of the He depth. This plot demonstrates that T_m is very nearly proportional to $N_s^{1/2}$ as expected for a phase boundary corresponding to a constant value of Γ . We find that $\Gamma = 137 \pm 15$ at the melting transition with the uncertainty arising primarily from the uncertainty in the He depth.⁸ To our knowledge, this constitutes the first experimental determination of a portion of the phase diagram for

an electron crystal.

The first calculation of the melting temperature for the classical 2D electron crystal was that by Platzman and Fukuyama.¹⁰ They employed an analytic calculation based on the self-consistent phonon method which yielded a melting transition near $\Gamma_m=3$. The first "computer experiment" on the classical 2D system was a molecular-dynamics calculation by Hockney and Brown¹¹ which revealed the melting transition near $\Gamma_m=95$. Though estimated $\Gamma_m=78$ using a dislocation model of melting.¹² A recent Monte Carlo calculation by Gann, Chakravarty, and Chester places the melting transition in the range $110 \lesssim \Gamma_m \lesssim 140$.¹³ This calculation is not inconsistent with our experimental result.

In this preliminary report, we have clearly left many questions unanswered. Topics such as the resonance linewidths, line shapes, and nonlinear effects were beyond the scope of this communication.

In conclusion, we have presented strong evidence that a classical 2D electron sheet crystallizes into a triangular lattice at low T and high N_s .

Among the numerous stimulating discussions that we have enjoyed with our friends and colleagues, we particularly want to acknowledge beneficial interactions with P. W. Anderson, T. R. Brown, A. J. Dahm, D. S. Fisher, B. I. Halperin, A. R. Hutson, D. Lambert, D. R. Nelson, P. M. Platzman, V. B. Shikin, and C. L. Zipfel. We thank R. C. Gann and G. V. Chester for a stimulating conversation and permission to mention one of their results prior to publication.

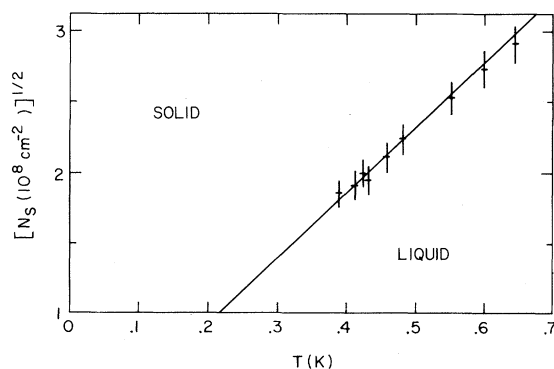


FIG. 2. Portion of the solid-liquid phase boundary for a classical, two-dimensional sheet of electrons. The data points denote the melting temperatures measured at various values of the electron areal density, N_s . Along the line, the quantity Γ , which is a measure of the ratio of potential energy to kinetic energy per electron, is 137.

¹E. P. Wigner, Phys. Rev. **46**, 1002 (1934).

²R. S. Crandall and R. Williams, Phys. Lett. **34A**, 404 (1971).

³For a recent review of electrons on He, see C. C. Grimes, Surf. Sci. **73**, 379 (1978).

⁴V. B. Shikin, Pis'ma Zh. Eksp. Teor. Fiz. **19**, 657 (1974) [JETP Lett. **19**, 335 (1974)].

⁵Yu P. Monarkha and V. B. Shikin, Zh. Eksp. Teor. Fiz. **68**, 1423 (1975) [Sov. Phys. JETP **41**, 710 (1976)].

⁶D. S. Fisher, B. I. Halperin, and P. M. Platzman, following Letter [Phys. Rev. Lett. **42**, 798 (1979)].

⁷The rf-driven element is a 75- Ω stripline laid out in a serpentine pattern over a circular area 2.5 cm in diameter. It is terminated in a 75- Ω resistor so the rf potential is essentially uniform over the whole driven element.

⁸The electron areal density is given by $N_s = (\epsilon V_u / 4\pi e d)$,

where $\epsilon = 1.057$ is the dielectric constant of liquid He. The He depth, d , is determined by measuring the capacitance between the guard ring and the top plate as the cell is filled. Because of capillary action and the meniscus, the uncertainty in d is $\approx \pm 10\%$.

⁹A square lattice, for example, would produce a resonance spectrum significantly different from that we observe. Furthermore, calculations show that the square lattice would have slightly higher energy than the triangular and would be dynamically unstable: G. Meissner,

H. Namaizawa, and M. Voss, Phys. Rev. B **13**, 1370 (1976); L. Bonsall and A. A. Maradudin, Phys. Rev. B **15**, 1959 (1977).

¹⁰P. M. Platzman and H. Fukuyama, Phys. Rev. B **10**, 3150 (1974).

¹¹R. W. Hockney and T. R. Brown, J. Phys. C **8**, 1813 (1975).

¹²D. J. Thouless, J. Phys. C **11**, L189 (1978).

¹³R. C. Gann, S. Chakravarty, and G. V. Chester, to be published.

Phonon-Ripplon Coupling and the Two-Dimensional Electron Solid on a Liquid-Helium Surface

Daniel S. Fisher and B. I. Halperin

Bell Laboratories, Murray Hill, New Jersey 07974, and Harvard University, Cambridge, Massachusetts 02138

and

P. M. Platzman

Bell Laboratories, Murray Hill, New Jersey 07974

(Received 17 January 1979)

We analyze the vibrational modes of a two-dimensional electron solid, coupled to the ripplon modes of a liquid-helium surface, as a function of temperature and external electric pressing field. Resonance observed experimentally by Grimes and Adams are thereby explained.

It has been expected for some time that electrons trapped just above a liquid-helium surface would form a triangular two-dimensional (2D) solid, at sufficiently low temperatures and high densities.^{1,2} Experimental demonstration of a phase transition in the trapped-electron system has been obtained by Grimes and Adams³ as described in the preceding Letter (hereafter referred to as GA). In the present Letter, we analyze the long-wavelength vibrational modes of the electron solid (phonons), taking into account their coupling with riplons (excitations of the helium surface). The resonances seen in GA are interpreted as arising from the low-lying longitudinal modes, at the discrete vectors \vec{q}_i determined by the geometry.

The vibrational frequency spectrum of the 2D electron solid, in the absence of coupling to riplons, has been given by several authors.² The transverse phonon branch has a linear frequency spectrum at long wavelengths, $\omega_i(q) = c_i q$ ($c_i = 0.245e^2n_s^{1/2}/m$ at $T=0$). Here e , m , and n_s are, respectively, the charge, mass, and areal num-

ber density of the electrons. Because of the long-range $1/r$ potential, the longitudinal-mode spectrum of the ideal electron crystal has the form of a 2D plasmon,⁴ $\omega_l = (2\pi n e^2 q/m)^{1/2}$. This spectrum is indicated by the dashed curve in Fig. 1.

The spectrum of riplons on an unperturbed helium surface, ignoring gravity, is given by $\Omega^2(\vec{K}) = \alpha K^3/\rho$, where α and ρ are the surface tension and density of the helium. The riplons of interest have wave vectors, $\vec{K} = \vec{G}_n + \vec{q}_i$, where \vec{G}_n is a reciprocal-lattice vector of the electron solid. For the triangular lattice, the magnitudes are given by $G_n^2 = nG_1^2$ ($n = 1, 3, 4, 7, 9, \dots$), where, neglecting possible vacancies and interstitials, $G_1^2 = 8\pi^2 n_s/3^{1/2}$. Since $q_i \ll G_n$, we may, in fact, consider Ω to be independent of \vec{q}_i . The lowest three ripplon frequencies $\Omega_n \equiv \Omega(G_n)$ are indicated by horizontal dashed lines in Fig. 1.

Consider a set of electrons at specified coordinates $\vec{r}(\ell) = \vec{R}(\ell) + \vec{u}(\ell)$ parallel to the surface, where $\vec{u}(\ell)$ is the horizontal displacement from the lattice position $\vec{R}(\ell)$. There will be a change in energy due to interaction with riplons, which we may write as⁵

$$H_I = S^{-1/2} (m\alpha/n_s)^{1/2} \sum_i \sum_{\vec{q}\vec{G}} \xi_{\vec{q}+\vec{G}} V_{\vec{q}+\vec{G}}^0 e^{i\vec{q}\cdot\vec{R}(\ell)} e^{i(\vec{q}+\vec{G})\cdot\vec{u}(\ell)}, \quad (1)$$